Demographic history shapes forest tree vulnerability to climate change

Thomas Francisco[1,*], Isabelle Lesur-Kupin[1], Carlos Guadaño-Peyrot[2], Sanna Olsson[2], Marija Kravanja[3], Marjana Westergren[3], Sara Pinosio[4], Thibaut Capblancq[5], Giovanni G. Vendramin[4], Katharina B. Budde[6], Lene R. Nielsen[7], James M. Doonan[7], Delphine Grivet[2], Elia Vajana[4], Juliette Archambeau[8], Andrea Piotti[4], Santiago C. González-Martínez[1,*]

[1]National Research Institute for Agriculture, Food and the Environment (INRAE), University of Bordeaux, UMR 1202 BIOGECO, 33610 Cestas, France

[2]Department of Forest Ecology and Genetics, Institute of Forest Sciences (ICIFOR-INIA), CSIC, Madrid, Spain

[3]Slovenian Forestry Institute, Večna pot 2, 1000, Ljubljana, Slovenia

[4]Institute of Biosciences and BioResources (IBBR), National Research Council (CNR), 50019 Sesto Fiorentino (Firenze), Italy

[5]Laboratoire d'Écologie Alpine, Université Grenoble Alpes, Université Savoie Mont-Blanc, CNRS, 38058 Grenoble, France

[6]Northwest German Forest Research Institute, Professor-Oelkers-Strasse 6, 34346 Hann. Münden, Germany

[7]Department of Geosciences and Natural Resource Management, University of Copenhagen, 1958 Frederiksberg C, Copenhagen, Denmark

[8]National Research Institute for Agriculture, Food and the Environment (INRAE), UMR 1391 ISPA, 88140 Villenave d'Ornon, France

*Corresponding authors:

Thomas Francisco (thomas.francisco@inrae.fr) and Santiago C. González-Martínez (santiago.gonzalez-martinez@inrae.fr)

INRAE UMR BIOGECO 1202,

DOMAINE DE L'HERMITAGE

69 Route d'Arcachon

33612 Cestas, France

ORCID Number

Thomas Francisco: 0009-0005-8618-0747, thomas.francisco@inrae.fr

Isabelle Lesur-Kupin: 0000-0001-7632-3955, isabelle.lesurkupin@inrae.fr

Carlos Guadaño-Peyrot: 0009-0007-8663-5216, carlospeyrot77@gmail.com

Sanna Olsson: 0000-0002-1199-4499, sanna.olsson@inia.csic.es

Marija Kravanja: 0009-0002-1478-6457, marija.kravanja@gozdis.si

Marjana Westergren: 0000-0002-4204-0161, marjana.westergren@gozdis.si

Sara Pinosio: 0000-0002-1820-3637, sara.pinosio@cnr.it

Thibaut Capblancq: 0000-0001-5024-1302, thibaut.capblancq@univ-grenoble-alpes.fr

Giovanni G. Vendramin: 0000-0001-9921-7872, giovannigiuseppe.vendramin@cnr.it

Katharina B. Budde: 0000-0002-5361-2815, katharina.budde@nw-fva.de

Lene R. Nielsen: 0000-0002-7214-8691, lron@ign.ku.dk

James Doonan: 0000-0002-0523-5808, jd@ign.ku.dk

Delphine Grivet: 0000-0001-8168-4456, dgrivet@inia.csic.es

Elia Vajana: 0000-0003-1340-3389, eliavajana@cnr.it

Juliette Archambeau: 0000-0003-0155-9538, juliette.archambeau@inrae.fr

Andrea Piotti: 0000-0002-3324-5325, andrea.piotti@cnr.it

Santiago C. González-Martínez: 0000-0002-4534-3766, santiago.gonzalez-martinez@inrae.fr

Abstract

Demographic history is expected to play a central role in shaping population vulnerability to climate change through its lasting effects on effective population sizes and genetic connectivity. However, existing studies report contrasting outcomes, and the consequences of alternative demographic histories have seldom been assessed concurrently across multiple taxa. Here, we analysed population genomic data from six of the major European forest tree species to address this gap. We found that, across all species, more genetically isolated populations showed reduced adaptive potential, as measured by standing levels of genetic diversity. Furthermore, populations with reduced historical gene flow and higher genetic differentiation exhibited higher genetic load and suboptimal climate adaptation, particularly in small, fragmented populations, potentially increasing their sensitivity to climate change. Finally, the beneficial effects of gene flow were evidenced by the absence of greater suboptimal climate adaptation in highly connected populations across the six species. Altogether, our results provide valuable insights into how genetic differentiation, reflecting the combined effects of genetic drift and limited historical gene flow, influences current vulnerability of forest tree populations to climate change.

Introduction

Trees are foundation species in many terrestrial ecosystems, supporting remarkable biodiversity, regulating the climate and providing other vital ecosystem services on a global scale[1]. Due to their long generation time and sessile nature, trees are particularly exposed to environmental hazards and gradual changes. An increasing body of literature indicates that they will not be able to adapt and/or disperse at rates matching projected climate change[2-4] and forests worldwide are already displaying signs of stress and decline[5,6]. The way in which populations respond to environmental changes depends on the intensity of the stress they experience, their sensitivity to this stress and their capacity to adapt to the new conditions, which together determine their vulnerability to a changing environment[7,8].

Genetic metrics are increasingly being used to assess vulnerability to climate change, as they capture impacts and responses at the intraspecific level[9-11]. Genetic diversity originates diverse phenotypes, some of which may confer advantages in shifting climate, thus forming the basis of the evolutionary potential of populations and, possibly, different patterns of local adaptation[12]. Although local adaptation is common in plants[13], the degree of local adaptation can be population-specific[14]. Both adaptation lags to current climate and pre-adaptation to future climate can influence the extent to which a population will be affected by climate change[15,16]. Recent advances in ecological genomics have introduced new metrics to quantify the extent of climate adaptation in populations (e.g., the genomic discrepancy index, GDI[17]). Genetic variation between populations resulting from different rates of accumulation and purging of deleterious mutations, can also shape their sensitivity to climate change. Indeed, levels of genetic load, defined as the reduction of fitness in a population due to deleterious mutations, can further constrain a population's ability to persist under shifting climatic pressures[18]. Additionally, inbreeding depression has been reported to be particularly high in gymnosperms compared to angiosperms[19,20], as evidenced, for example, by the high number of lethal equivalents affecting tree fitness observed in conifers[20-24]. Overall, regardless of their impact on

current fitness or adaptive potential, population attributes such as genetic diversity, climate adaptation, or genetic load are shaped by demographic processes, and are therefore neither static through time nor uniform across populations[23-27].

Over evolutionary timescales, tree populations have been profoundly shaped by repeated glacial cycles, large-scale environmental shifts and, more recently, land-use changes. These events triggered large distributional shifts that came with important variation in population size and connectivity, and thereby shaped the genetic makeup of populations. The impact of demographic history on wild populations is widely recognised, primarily through its effects on effective population sizes, gene flow and range limits[26,28,29]. However, its overall impact on tree species' genetic diversity remains unclear and requires broader investigation across species with contrasting demographic histories[30]. Demographic history can also affect a population's potential for climate adaptation by influencing the amount of standing genetic variation available for natural selection and the patterns of adaptive or maladaptive gene flow[31-33]. Furthermore, genetic load is also impacted by demographic historical events, through the purging or accumulation of deleterious mutations[24,25]. Although well-established theoretical predictions on the link between demographic history and genetic load exist[34,35], empirical studies have reported contrasting results[36-39], highlighting the need for further research, particularly in forest trees.

In this study, we investigated how historical demographic processes may have shaped key components of population vulnerability, namely sensitivity and adaptive potential, in six ecologically and economically important tree species: four conifers (*Taxus baccata* L., *Pinus pinea* L., *Pinus pinaster* Ait. and *Pinus sylvestris* L.) and two angiosperms (*Fraxinus excelsior* L. and *Fagus sylvatica* L.). By integrating genomic data from 6,434 trees across 326 populations spanning most of the species' distributions in Europe and surrounding regions, we estimated genetic diversity, genetic load, and current climate adaptation, and related these metrics to population-level genetic differentiation, used here as a proxy for demographic history. Finally, we interpreted these associations in the light of how historical demographic processes, including genetic drift and population isolation, may have

117 influenced present-day sensitivity and adaptive potential to ongoing climate change.

118

119 *Results*

120 *Population genetic differentiation reflects the species' demographic history*

121 The six tree species included in this study were chosen to follow a range of typical population sizes
122 and levels of connectivity, likely resulting from the interplay between life-history traits and
123 contrasting demographic histories. Population-level genetic differentiation (F_{ST}) reflected well these
124 patterns (Fig. 1). Populations of *T. baccata* and *P. pinea* consistently showed intermediate to high F_{ST}
125 (median values of 0.151 and 0.380, respectively; higher than any other species), which may have
126 arisen from their known reduced effective population size and connectivity, resulting from recurrent
127 historical bottlenecks and long-term habitat contraction[40-42]. In contrast, *P. pinaster*, displayed
128 greater variability in F_{ST} across populations, reflecting the presence of continuous and well-connected
129 populations in parts of its range, as well as smaller and fragmented ones in other parts, likely
130 resulting from contractions during glacial periods followed by post-glacial range expansions and
131 reduced gene flow across gene pools[30,43]. Finally, *F. excelsior*, *F. sylvatica* and *P. sylvestris* populations
132 displayed very low F_{ST}, with only a few populations showing higher genetic differentiation (e.g., F_{ST} >
133 0.2 only in two *F. excelsior* and one *P. sylvestris* populations). Most populations of these species are
134 known to be well-connected due to a combination of factors such as multiple glacial refugia,
135 extensive post-glacial expansion and admixture, notable cold tolerance and efficient long-distance
136 gene flow[19,30,43-51]. Nevertheless, smaller, fragmented populations can sporadically be found in few,
137 mainly southern, parts of the range of these species due to environmental constraints or
138 geographical barriers (*F. excelsior*[48]; *F. sylvatica*[52]; reviewed in Pyhäjärvi *et al*.[19] for *P. sylvestris*).

139 In addition, the geographical distribution of population-level F_{ST} varied among species. Highly
140 differentiated populations of *T. baccata* and *P. pinea* showed no clear spatial pattern (Fig. 1A, B),

141 with high F_{ST} even in populations located within the species' core range. In contrast, the other species
142 exhibited higher F_{ST} towards the range edges compared to their core populations (Fig. 1C-F; see also
143 Theraroz *et al*.[39] and Guadano-Peyrot *et al*.[53]).

144 *Key intraspecific components of climate change vulnerability vary across populations and*
145 *species*

146 Genetic diversity (*H*s) varied considerably within species, with distinct patterns emerging across
147 species (Fig. 2A; but notice that direct comparisons of genetic diversity among species are not
148 appropriate due to the use of different genotyping platforms; see Methods). At the within-species
149 level, *P. pinea* exhibited the greatest among-population variability in *H*s, as evidenced by its relatively
150 flat cumulative curve compared with the other species. The other two pine species also had higher
151 among-population variability in *H*s than *T. baccata* and the two broadleaves, for which the cumulative
152 curves were steeper. *H*s changed significantly with longitude in most species, increasing eastward in
153 *T. baccata*, *F. sylvatica* and *P. sylvestris*, decreasing in *P. pinea* and *P. pinaster* and showing no
154 significant trend in *F. excelsior* (Fig. S2A; Table S1). Additionally, *H*s increased significantly with
155 latitude in *P. pinaster* and *P. sylvestris*, with southern range-edge populations of both species
156 showing lower genetic diversity (Fig. S2B). These patterns likely reflect known glacial and post-glacial
157 forest dynamics as reconstructed from genetic data and pollen records (e.g.,[39,42,44,54-58]).

158 We also observed marked differences in realised genetic load (i.e., estimated by the number of
159 deleterious mutations in the homozygous state; hereafter referred to as 'genetic load'; see Methods)
160 among species (Fig. 2B). Interestingly, *P. pinea* exhibited the highest genetic load values, whereas *T.*
161 *baccata*, *P. pinaster* and *P. sylvestris* had comparable lower medians (although *P. sylvestris* showed a
162 slightly higher genetic load than *P. pinaster* and *T. baccata* showed intermediate values).
163 Furthermore, among-population variability in genetic load was larger in *P. pinea* and *P. pinaster* than
164 in *T. baccata* and *P. sylvestris* (e.g., 0.074 to 0.150 in *P. pinaster* compared to 0.109 to 0.126 in *P.*
165 *sylvestris*).

166 Using the best genotype-environment association (GEA) models, we selected candidate single
167 nucleotide polymorphisms (SNPs) to estimate climate adaptation via the genomic discrepancy index
168 (GDI; corresponding to the deviation of a population from the expected GEA models; see Methods),
169 retaining between 100 (*T. baccata*) and 2,957 (*F. excelsior)* SNPs depending on the species (Figs. 2C,
170 S3; Table S2). The distribution of GDI (Fig. 2D) showed considerable variability within and among
171 species. The distributions for *F. sylvatica* and *P. pinaster* were nearly Gaussian, whereas *F. excelsior*
172 *and P. sylvestris* were still roughly Gaussian but exhibited long tails with higher GDI values. In
173 contrast, *T. baccata* and *P. pinea* displayed very long tails of higher GDI values, approaching a
174 bimodal distribution, with many populations exhibiting elevated GDI. Populations of *T. baccata* with
175 high GDI are primarily found in southern regions, including Greece, Bosnia-Herzegovina, Spain and
176 Italy[17].

177 *Population genetic differentiation as a major factor explaining key components of climate*
178 *change vulnerability*

179 Genetic diversity (*H*s) decreased with increasing population-level genetic differentiation (F_{ST}) in all
180 species (Table 1), a pattern that was further confirmed by using unbiased Jost's D (Table S3; see
181 Methods). Associations remained highly significant and consistent across species when atypical
182 population-level F_{ST} values were removed and when geography was considered in the models (except
183 for *F. excelsior*; Table 1; Fig. S4; see Methods).

184 Associations between genetic load and population-level F_{ST} varied among species, exhibiting
185 accumulation, purging or no change in load as F_{ST} increased. These relationships were also influenced
186 by whether populations with atypically high population-level F_{ST} values were included or not in the
187 analysis (Table 1; Figs. 3A, S5A). We identified three main groups of species, which mirrored their
188 positions along the population size and connectivity gradient (Fig. 1G). First, *T. baccata* and *P. pinea*
189 consistently exhibited higher genetic load (i.e., higher accumulation of deleterious mutations in
190 homozygosis) in populations with higher F_{ST}, irrespectively of whether atypical populations were

191 included or not. Remarkably, *P. pinaster* showed the opposite pattern, with higher genetic load
192 (whether including or excluding atypical populations) in populations with lower F_{ST}. Finally, *P.*
193 *sylvestris* showed either a non-significant association when including atypical populations or a
194 marginally significant negative association without them (as *P. pinaster*). Genetic load was not
195 computed for the two broadleaves (*F. excelsior* and *F. sylvatica*) as its impact is expected to be lower
196 in angiosperm species (see Introduction).

197 Climate adaptation, assessed via GDI, also varied among species in ways that reflected the
198 population size and connectivity gradient illustrated in Fig. 1G, with higher genetic differentiation
199 having from negative to negligible effects on climate adaptation along this gradient (Table 1; Fig. 3B,
200 S5B). In *T. baccata* and *P. pinea*, patterns mirrored those observed for genetic load, with higher GDI
201 in populations exhibiting greater F_{ST}. A similar pattern was observed in *P. pinaster*, *F. excelsior* and *F.*
202 *sylvatica*, although for the latter two species it was only evident when populations with atypically
203 high population-level F_{ST} were included, likely reflecting higher thresholds of isolation required to
204 affect climate adaptation. Finally, no significant association was detected between population-level
205 F_{ST} and GDI in the widespread, weakly differentiated *P. sylvestris*.

206

207 *Discussion*

208 Our study suggests that, beyond macro-glacial dynamics, local historical events and demography, as
209 reflected in present-day genetic differentiation, explain a substantial portion of the variability in
210 genetic diversity among populations. We consistently observed a reduction in genetic diversity with
211 increasing population-level F_{ST}. This result remained robust after accounting for geographic effects
212 (Table 1), except for *F. excelsior*. Since geography has previously been linked to glacial-postglacial
213 dynamics[59], these findings support the additional role of local genetic drift and limited historical gene
214 flow in shaping the observed patterns. Overall, our work suggests that even species capable of long-
215 distance dispersal and therefore substantial gene flow may still experience long-term isolation. This

216 isolation likely led to reduced genetic diversity through a combination of ecological or environmental
217 specialisation, genetic drift, and inbreeding[30,60,61]. Since rapid adaptation mostly relies on standing
218 genetic variation[62], the general reduction in genetic diversity in highly differentiated populations
219 could limit their adaptive potential, making them particularly vulnerable to climate change[12,39].

220 The relationship between genetic differentiation and genetic load varied across species, reflecting
221 their specific life-history traits and demographic histories. The accumulation of deleterious mutations
222 in highly differentiated populations of *T. baccata* and *P. pinea* was consistent with their life-history
223 traits, spatial distribution and demographic history. Populations of these species are often small and
224 fragmented, and in *T. baccata*, dioecy further reduces effective population size[41,42]. Under such
225 conditions, historical isolation can amplify genetic drift, further reducing the effective population size
226 and increasing inbreeding. This can increase the fixation rates of deleterious alleles, weaken purifying
227 selection and ultimately decrease population fitness[64-66]. Similar patterns have been reported in
228 other long-lived organisms, where isolation and reduced gene flow have exacerbated the
229 accumulation of deleterious mutations in small populations, likely constraining their adaptive
230 potential[66,67].

231 The contrasting patterns observed in *P. pinaster* (negative association) and *P. sylvestris* (no
232 association) can also be explained by past differences in population size and connectivity. Historically
233 large and well-connected *P. sylvestris* populations likely homogenised the distribution of deleterious
234 mutations across populations (average population F_{ST} of 0.05; see also Fig. 1F), explaining both the
235 absence of a statistically significant relationship between population genetic differentiation and
236 genetic load, and the low variance observed among populations (Fig. 2B). This interpretation is
237 supported by other studies showing no discernible signal of higher genetic load in expanding
238 populations of this species[68]. The negative relationship observed in *P. pinaster* may, however, reflect
239 more efficient purging of deleterious mutations in historically isolated populations that are part of
240 relatively large, dynamic gene pools, as discussed in Slotte *et al*.[69]. Present-day gene pools in *P.*
241 *pinaster* are known to have originated from multiple refugia with relatively stable population sizes,

242 which may have enhanced the efficacy of purifying selection by reducing genetic drift[39]. Combined
243 with limited gene flow across refugia, this could have led to a higher removal of deleterious alleles in
244 refugial populations[37,65,70,71].

245 Overall, demographic history, underlying population genetic differentiation, accounted for a
246 substantial part of the variation in genetic load across conifer populations. In particular, the strength
247 and direction of the significant associations in our study appeared to depend on factors such as
248 historical effective population size and connectivity. Accounting for these factors is therefore
249 essential to correctly interpreting how demographic history shapes the accumulation and effects of
250 deleterious mutations, which may in turn compromise population persistence under climate change.

251 Increasing genetic differentiation was associated with suboptimal climate adaptation in all species
252 except *P. sylvestris*. Alongside the parallel reduction in genetic diversity with increasing
253 differentiation, these results highlight the potential beneficial role of gene flow in enhancing
254 adaptation by maintaining standing genetic variation, a key driver of adaptive evolution[33,64].
255 Furthermore, both theoretical predictions and empirical evidence also showed that, by introducing
256 pre-adapted alleles, gene flow can further facilitate climate tracking, particularly in leading-edge
257 populations[32,72,73]. We observed marked interspecific differences in climate adaptation in our study.
258 Species with a prevalence of small and fragmented populations (e.g., *T. baccata* and *P. pinea*)
259 showed stronger negative associations between population genetic differentiation and climate
260 adaptation than species with larger, more continuous populations (e.g., *F. sylvatica* and *P. sylvestris*).
261 These differences may, at least in part, reflect variation in historical effective population size, as the
262 benefits of increased standing genetic diversity and enhanced climate tracking via gene flow are
263 likely to be more pronounced in smaller populations[32,73,74].

264 Interestingly, across the six tree species, populations with low genetic differentiation consistently
265 showed no signs of reduced climate adaptation. These results provide further empirical support for
266 the positive role of genetic connectivity in enhancing climate adaptation in small, fragmented

267 populations, while showing no detectable negative effects in larger, more continuous populations.
268 However, while biologically meaningful, these insights need to be taken with caution. For instance,
269 climate adaptation models used here rely on several assumptions, including that genotype-
270 environment associations accurately capture adaptive signals[75]. Furthermore, higher Euclidean
271 distances between observed and predicted genomic compositions (GDI) were interpreted here as
272 signatures of suboptimal climate adaptation, therefore neglecting other potential explanations, such
273 as alternative adaptive pathways or pre-adaptation to future climate.

274

275 *Conclusion*

276 Genomic analyses of 6,434 trees from 326 populations across six ecologically and economically
277 important forest tree species revealed major effects of demographic history, as summarised by
278 population-level genetic differentiation, on shaping population vulnerability to climate change.
279 Population adaptive potential, as measured by within-population genetic diversity, declined
280 consistently with historical isolation. At the same time, increased population sensitivity to climate
281 change, through the accumulation of genetic load and suboptimal climate adaptation, was likely
282 driven by reduced historical gene flow in species with a prevalence in small, fragmented populations.
283 No such effects were detected in species with larger, more connected populations, except for a few
284 populations that exhibited atypically high genetic differentiation. Overall, this work provides valuable
285 insights into how genetic differentiation, reflecting genetic drift and limited historical gene flow,
286 influences current vulnerability of forest tree populations to climate change. Future empirical work
287 could aim to link genetic metrics to effective population size, phenotypic performance, or
288 reproductive fitness, to better assess the contribution of each factor to climate vulnerability. Our
289 findings can also inform management strategies, including assisted gene flow, by helping to identify
290 populations most at risk from climate change and those likely to benefit from increased genetic
291 variance in fitness-related traits[76]. Assessing current gene flow dynamics will be crucial to determine

292 whether rapid environmental change is already reshaping historical patterns of connectivity and
293 genetic differentiation.

294

295 *Materials and methods*

296 *Sampling and genotyping*

297 Our study focused on six European tree species, namely *Taxus baccata*, *Pinus pinea*, *Pinus pinaster*,
298 *Fraxinus excelsior, Fagus sylvatica* and *Pinus sylvestris.* Species were selected to represent
299 contrasting demographic histories, including different phylogenetic groups, stand formation and
300 population sizes, as well as levels of connectivity and population genetic structure[30,43] (Fig. 1G; see
301 Results). For each species, 29-86 populations spanning most of their ranges were sampled, with total
302 sample sizes per species ranging from 490 to 1,728 mature trees (except *for F. excelsior* where young
303 trees were sampled; see Supplementary Files 1 and 2). Particular attention was paid to sample
304 populations with different degrees of genetic differentiation, including both core and range-edge
305 populations.

306 Genomic data for 490 trees representing 29 populations of *T. baccata* were obtained from a previous
307 study[17]. This dataset comprised single nucleotide polymorphisms (SNPs) generated by combining
308 gene-capture and single-primer enrichment technology (SPET) data.

309 Genomic data for 461 trees from 31 natural populations of *F. excelsior* were compiled from one
310 previous data paper and one study: 286 trees sequenced using SPET[77] and 175 using low-coverage
311 whole genome sequencing[78], following Doonan *et al*.[79]. SNPs were called against the same reference
312 genome, FRAX_0001_PL[80].

313 Genomic data for 1,224 trees from 51 populations of *F. sylvatica* were generated by combining two
314 previous datasets: 370 trees from a data paper[77] and 864 trees from a published dataset[81], both of

315 which produced using SPET. SNP quality filtering and the removal of outliers and duplicates were
316 performed on the merged dataset following the procedure described in Pinosio *et al*.[77].

317 Genomic data for the three pine species (*P. pinea*: 952 trees from 48 populations; *P. pinaster*: 1,579
318 trees from 86 populations; *P. sylvestris*: 1,728 trees from 81 populations) were retrieved: from a
319 previous study[82] for *P. pinaster* and from a data paper[83] for *P. pinea* and *P. sylvestris*. SNP genotypes
320 were generated using the multispecies 4TREE (*P. pinea*, *P. pinaster*) and the PiSy50k (*P. sylvestris*)
321 Axiom arrays (Thermo Fisher Scientific, USA) at IGA Technology Services (Udine, Italy). Following
322 Olsson *et al*.[83], we applied the quality thresholds for markers CR ≥ 85, FLD ≥ 3.2, HetSO ≥ -0.3 and
323 samples DQC ≥ 0.4 with QC call rate ≥ 85, in order to maximise SNP retention while ensuring high
324 data quality.

325 Overall, genomic datasets included 6,434 trees from 326 populations, mainly in Europe and
326 bordering regions in North Africa and Asia (see details in Supplementary Files 1 and 2). For each
327 species, we performed population genetic structure analyses to ensure that merged datasets were
328 biologically consistent and appropriate for downstream analyses (Figs. S6, S7). Two of the 326
329 populations (COM and FUEbis of *P. pinaster*) were excluded because they were duplicated or had too
330 few samples. For each species, two datasets were then generated after removing monomorphic SNPs
331 and variants that failed additional filtering thresholds (coverage depth < 7 or > 150, and allele
332 balance at heterozygous sites < 0.2 or > 0.8). The first dataset (*dataset 1*) retained SNPs and
333 individuals with less than 15% missing data and SNPs with a minor allele count of at least three
334 (except for *T. baccata*, see Francisco *et al*.[17]). This dataset was used for population genetic structure
335 (PCA, STRUCTURE) and differentiation (population-level F_{ST}) analyses, as well as for calculating
336 genetic diversity (*H*s), as these analyses are sensitive to high rates of missing data and low-frequency
337 SNPs[84]. *Dataset 1* comprised between 3,563 (*P. pinea*) and 34,760 SNPs (*P. sylvestris*), depending on
338 the species, with a total of 6,262 trees genotyped across the 324 populations (Table S4). The second
339 dataset (*dataset 2*), used for computing climate adaptation and genetic load statistics, was filtered
340 out for missing data > 30% (both for SNPs and individuals) and for minor allele counts lower than

341 twice the number of individuals in the smallest population before filtering (Table S4). This latter filter
342 was applied to remove low-frequency alleles that could otherwise increase false-positive rates, while
343 retaining potential climate-associated SNPs or deleterious mutations that are fixed in small
344 populations. *Dataset 2* included between 3,790 (*P. pinea*) and 34,848 SNPs (*P. sylvestris*), depending
345 on the species, with a total of 6,326 trees genotyped across the 324 populations (Table S4). From
346 these datasets, SNPs from coding regions that could be polarised and annotated using the *Pinus*
347 *tabuliformis* or *Taxus chinensis* reference genomes[85,86] were used to estimate genetic load (see
348 below). This yielded 4,703; 1,195; 2,253; and 13,221 SNPs for *T. baccata*, *P. pinea*, *P. pinaster*, and *P.*
349 *sylvestris*, respectively. Finally, for climate adaptation analyses, missing data in *dataset 2* were
350 imputed using the most common genotype within each gene pool.

351 *Climatic data*

352 Climatic data were extracted at high spatial resolution (30 arc-seconds) from Climate Downscaling
353 Tool (ClimateDT[87]). The 1901-1950 period was defined as the reference climate to which the
354 populations are currently adapted, except for *F. excelsior*, for which the 1991-2020 period was used
355 instead. This more recent time interval may better reflect the climate to which populations are
356 adapted in this species, given the relatively young age of the sampled trees and the species' known
357 capacity for rapid adaptation[88]. For each species, the retained climatic variables (Table S5) were
358 selected following the approach described in Francisco *et al.*[17]: (i) a pre-selection step based on
359 species life-history traits and the available literature, (ii) forward selection analysis based on genomic
360 importance, and (iii) removal of correlated variables (Pearson's $|r| > 0.75$) to ensure that
361 multicollinearity remained low and the variance inflation factor below 10 across variables (see
362 Supplementary Material).

363 *Population genetic structure and differentiation*

364 For each species, principal component analysis (PCA) was used to assess population genetic
365 structure, as implemented in the VEGAN R package[89] (Fig. S6). Genetic clusters were also examined

366 based on previously[17,90] or newly run Bayesian clustering analyses, as implemented in STRUCTURE
367 v2.3.4[91] (Fig. S7). For newly run STRUCTURE analyses, ten independent MCMC runs were performed
368 for each number of potential clusters (K = 1-10), with 100,000 iterations per run and a burn-in of
369 10,000 iterations. The most probable number of genetic clusters was determined using the ΔK
370 method[92].

371 Population-level genetic differentiation (F_{ST}), used here as a proxy for population-specific
372 demographic history, encompassing historical population size fluctuation, gene flow and connectivity
373 (e.g.,[93,94]), was calculated using BayeScan v2.1[95]. In this approach, F_{ST} represents the genetic
374 differentiation of each population relative to a predicted ancestral gene pool, making it less
375 influenced by local outliers and more reflective of broad historical patterns of divergence. Given the
376 comprehensive sampling effort, including both core and range-edge populations for each species,
377 populations with high F_{ST} can be considered more historically isolated than the species average.

378 *Genetic metrics of vulnerability to climate change*

379 Genetic differences among individuals of the same species can produce diverse phenotypes within
380 populations, some of which may confer advantages in shifting climate. The extent of this genetic
381 diversity can determine the population's evolutionary potential[12]. Genetic variation within
382 populations was quantified using Nei's genetic diversity (*H*s), as implemented in the HIERFSTAT R
383 package[96]. Due to the differences in experimental design to obtain genomic data (e.g., gene capture,
384 SPET designs and different genotyping arrays), genetic diversity values cannot be compared across
385 species.

386 Genetic load was estimated only for the conifer species in this study (*T. baccata*, *P. pinea*, *P. pinaster*,
387 and *P. sylvestris*), as the accumulation of deleterious mutations in these species has been shown to
388 be greater than in broadleaves and linked to fitness-related traits (e.g.,[97]; see Introduction). First,
389 SNPs were mapped onto the *Pinus tabuliformis* reference genome[85] (*P. pinea*, *P. pinaster* and *P.*
390 *sylvestris*; see Supplementary Material) or onto the *Taxus chinensis* reference genome[86] (*T. baccata*).

391 SnpEff software (version 5.1) was then used to identify SNPs causing amino acid changes in protein-
392 coding sequences[98]. Finally, the functional impact of mutations was predicted using PROVEAN
393 (version 1.1.5), a software that assesses the impact of mutations by evaluating sequence
394 conservation and alignment scores across homologous proteins[99]. For each SNP, PROVEAN predicted
395 its impact on the biological function of the corresponding protein and assigned a 'deleteriousness'
396 score. Mutations were considered deleterious when the PROVEAN score was lower than -2.5[99].
397 Realised genetic load was then computed following González-Martínez *et al*.[27], as the ratio of the
398 expected number of deleterious mutations in homozygosis to the number of expected neutral
399 mutations. As most deleterious alleles are thought to be recessive, the realised genetic load is
400 therefore expected to have a stronger immediate impact on fitness than the absolute number of
401 deleterious mutations[27,65].

402 Population climate adaptation was quantified using a two-step procedure. First, we investigated the
403 presence of genomic markers potentially involved in climate adaptation by carrying out genotype-
404 environment association (GEA) analyses. For each species, six GEA methods (correcting or not for
405 population genetic structure) were applied to identify candidate loci: redundancy analysis (RDA),
406 partial redundancy analysis (pRDA), latent factor mixed models (LFMM), BayPass, gradient forest (GF)
407 uncorrected for population genetic structure (GF-raw) and GF corrected for population genetic
408 structure (GF-corrected; see Table S6 and Supplementary Material for details). We then defined an
409 *all-outlier* SNP set comprising all candidate SNPs identified across the GEA analyses. Following
410 Archambeau *et al*.[100], an *outlier* SNP set was further defined, including only unlinked candidate SNPs
411 identified by at least two GEA methods. For this, we used a linkage disequilibrium threshold of R^2 <
412 |0.7| within contigs or 2,000 bp, depending on the available information for each species, and
413 filtered the datasets for linked loci using the GENETICS R package[101]. For each species, a *random* SNP
414 set was also generated by randomly selecting SNPs not identified as candidates by any GEA method,
415 matching both the number and allele frequency distribution of the *outlier* set (see Supplementary
416 Material).

417 Second, climate adaptation was quantified for each population within species by computing the
418 genomic discrepancy index (GDI[17]) using the RDA method. GDI computes the Euclidean distances
419 between the observed and predicted population scores along the retained RDA axes. Higher
420 population GDI indicates a greater deviation from the established GEA relationship relative to other
421 populations. For most species, the *all-outlier* SNP set was used to build the reference GEA model for
422 GDI estimates. However, for *T. baccata* and *P. pinaster*, we applied SNP sets (*random* and *outlier*,
423 respectively) previously identified as most suitable through model evaluation with fitness
424 proxies[17,100].

425 For all species, GDI estimates based on alternative SNP sets were highly correlated with those
426 obtained from the selected sets (Pearson's correlation > 0.64; Table S2).

427 *Linking demographic history to vulnerability to climate change*

428 To assess the effects of demographic history on population vulnerability to climate change, we
429 examined, for each species, the relationship between population-level F_{ST} and genetic diversity,
430 genetic load and GDI (see Supplementary File 3). Associations were evaluated using linear models
431 with *F*-test *p*-values, as implemented in the STATS R package[102]. To avoid interpreting associations
432 driven solely by extreme values, linear models were investigated with and without populations
433 exhibiting atypically high F_{ST}, defined as those falling outside 2.4 times the interquartile range of
434 population-level F_{ST} within each species.

435

436 *Author Contributions*

437 Designed research: TF, AP, SCG-M; acquired and pretreated genomic data: SO, MK, MW, SP, GGV,
438 KBB, LRN, JMD, DG, EV; analysed data: TF, IL-K; wrote the paper: TF, SCG-M; obtained funding: MW,
439 GGV, DG, AP, SCG-M, LRN; all authors participated in discussions and revised multiple versions of the
440 manuscript, including the final version.

Acknowledgments

TF was funded by a PhD grant of the INRAE Scientific Department ECODIV. EV was supported by the MSCA European fellowship MedForAct (GA 101107604). MK was supported by the Slovenian Research Agency (research core funding no. P4-0107 and Young Researcher grant no. 58170). This research was funded by EU H2020 FORGENIUS (grant agreement No. 862221) and Horizon Europe OptFORESTS (grant agreement No. 101081774) projects. Views and opinions expressed are however those of the authors only and do not necessarily reflect those of the European Union. Neither the European Union nor the granting authority can be held responsible for them. Additional *F. excelsior* data was generated by the AshAdapt project supported by the Independent Research Fund Denmark (DFF Technology and Production Sciences) under grant no. 8022-00355B. We are grateful to the Genotoul bioinformatics platform Toulouse Occitanie (Bioinfo Genotoul, https://bioinfo.genotoul.fr/) for providing computing and storage resources.

Data Archiving Statement

Genomic data for *Taxus baccata* from Francisco *et al*.[17] is available at Data INRAE (doi: https://doi.org/10.57745/JJ0ZEI); for *Pinus pinaster* from Olsson *et al*.[82] at Zenodo (doi: 10.5281/zenodo.14950394); for *Pinus pinea* and *Pinus sylvestris* from Olsson *et al*.[83] at Zenodo (doi: 10.5281/zenodo.17455887 and 10.5281/zenodo.17462035, respectively). Newly combined genomic data for *Fraxinus excelsior* and *Fagus sylvatica* are openly available at Data INRAE (doi: 10.57745/OG2FBY).

Code availability

Code used for data processing and analysis will be made publicly available upon publication at a GitHub public repository.

Table and Figures

Table 1. **Association between population genetic differentiation (F_{ST}) and genetic diversity (*Hs*)**. Linear model coefficient signs (β), explained variance (R^2), and *F*-test *p*-values, summarising the direction and strength of the relationship between population-level F_{ST}, used here as a proxy for demographic history, and genetic diversity (*Hs*). Analyses were run including and excluding populations exhibiting atypically high F_{ST} values and accounting or not for geographical variation in *Hs* (longitude 'Lon' and latitude 'Lat').

Species	***Excluding atypical populations***		***Including atypical populations***	
	***Hs* ~ F_{ST}**	***Hs* ~ F_{ST} | Lon + Lat**	***Hs* ~ F_{ST}**	***Hs* ~ F_{ST} | Lon + Lat**
T. baccata	(-) 0.59***	(-) 0.51***	(-) 0.59***	(-) 0.51***
P. pinea	(-) 0.87***	(-) 0.70***	(-) 0.87***	(-) 0.70***
P. pinaster	(-) 0.46***	(-) 0.24***	(-) 0.52***	(-) 0.28***
F. excelsior	(-) 0.13^{m}	(-) 0.12^{m}	(-) 0.43***	(-) 0.33***
F. sylvatica	(-) 0.56***	(-) 0.50***	(-) 0.88***	(-) 0.71***
P. sylvestris	(-) 0.33***	(-) 0.31***	(-) 0.48***	(-) 0.40***

$^{m:}$ $0.10 < p < 0.05$; ***: $p < 0.001$

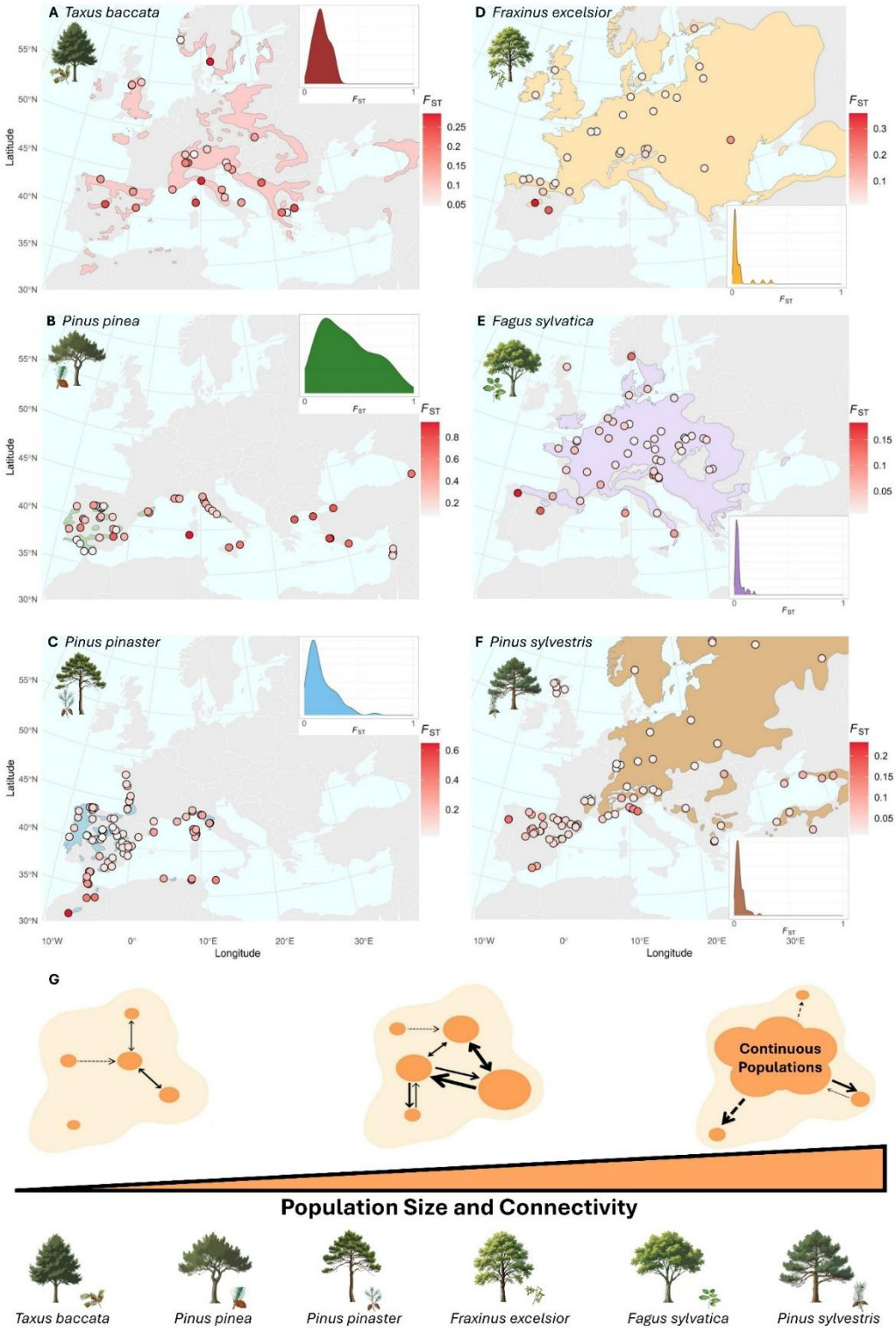

Figure 1. **Description of the six tree species**. **A-F** Geographical range and population-level genetic differentiation (F_{ST}). Each circle represents a population, with colour intensity indicating the magnitude of F_{ST}. Inserts show the density distribution of population-level F_{ST} values, represented on

481 a common scale to facilitate visual comparison across species. Shaded areas depict the approximate
482 species range[103] for the geographic extent of latitude 30°N-60°N and longitude 10°W-37°E. Sampled
483 populations of *P. sylvestris* occurring outside this range are not shown but can be found in Fig. S1.
484 Notice that species such as *T. baccata*, despite having a large geographical range, have a scattered
485 distribution while others (e.g., *P. sylvestris*) constitute large, stand-forming populations. **G** Conceptual
486 illustration of the gradient in population size and connectivity represented by the six species under
487 study[30,40-43,46,50], which spans from species with predominantly small and isolated populations to
488 species with large and well-connected populations. The schematic is inspired by[43].

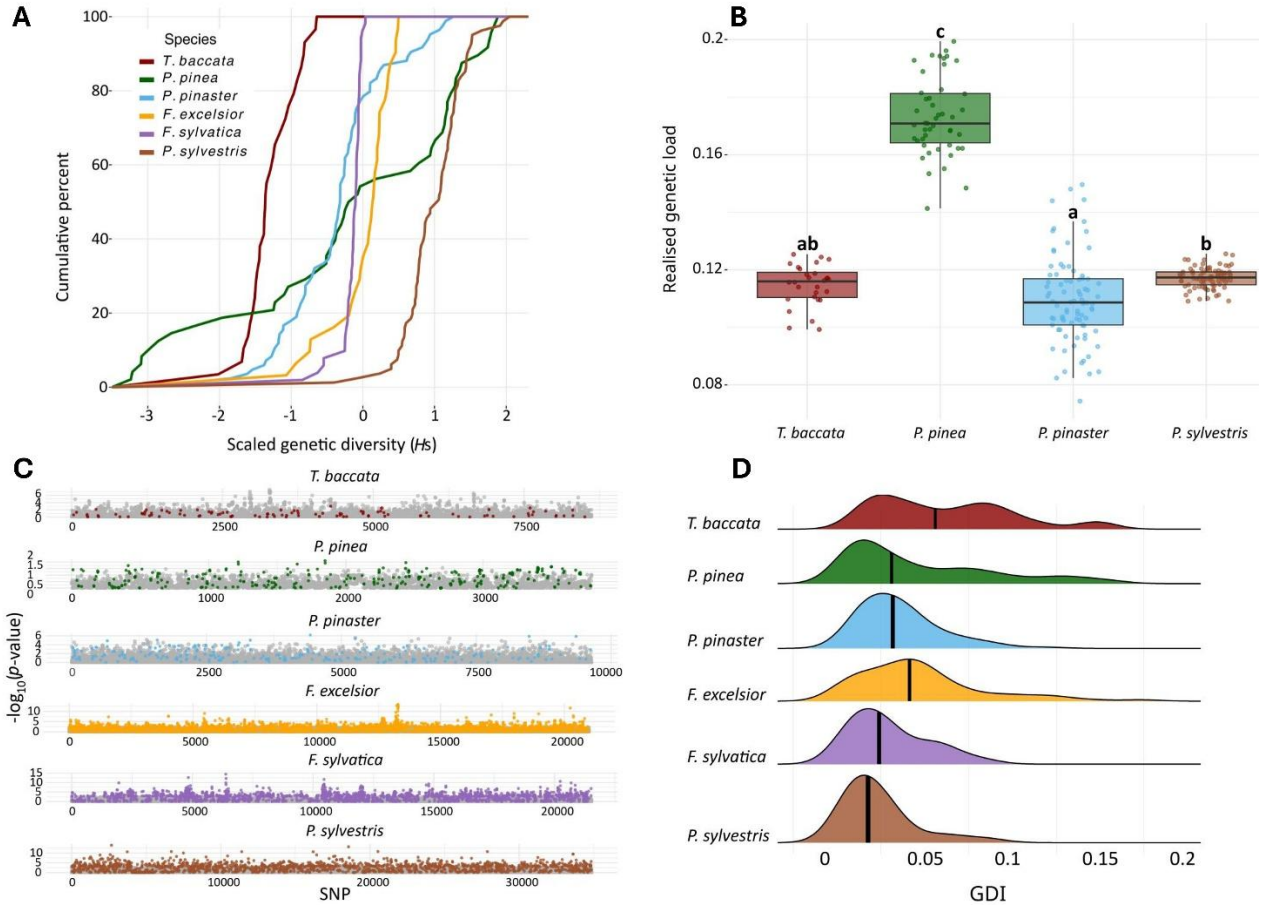

Figure 2. **Genetic metrics of population vulnerability to climate change across the studied species**. **A** Cumulative distribution of scaled genetic diversity (*Hs*; calculated by subtracting the mean and dividing by the standard deviation) across populations. A stepped curve indicates low variability in *Hs* across populations (e.g., *F. sylvatica*), whereas a flatter curve indicates high variability (e.g., *P. pinea*). **B** Comparison of realised genetic load across the four conifers species, with Tukey post-hoc groups indicated by lowercase letters. **C** Manhattan plots showing the retained candidate SNPs (coloured) used for GDI calculation, plotted against the total number of SNP, which varied across species (Table S2). *P*-values were obtained from the RDA GEA models. **D** GDI density plot across populations for each species. Black line represents the median GDI values. Note that values are not directly comparable among species.

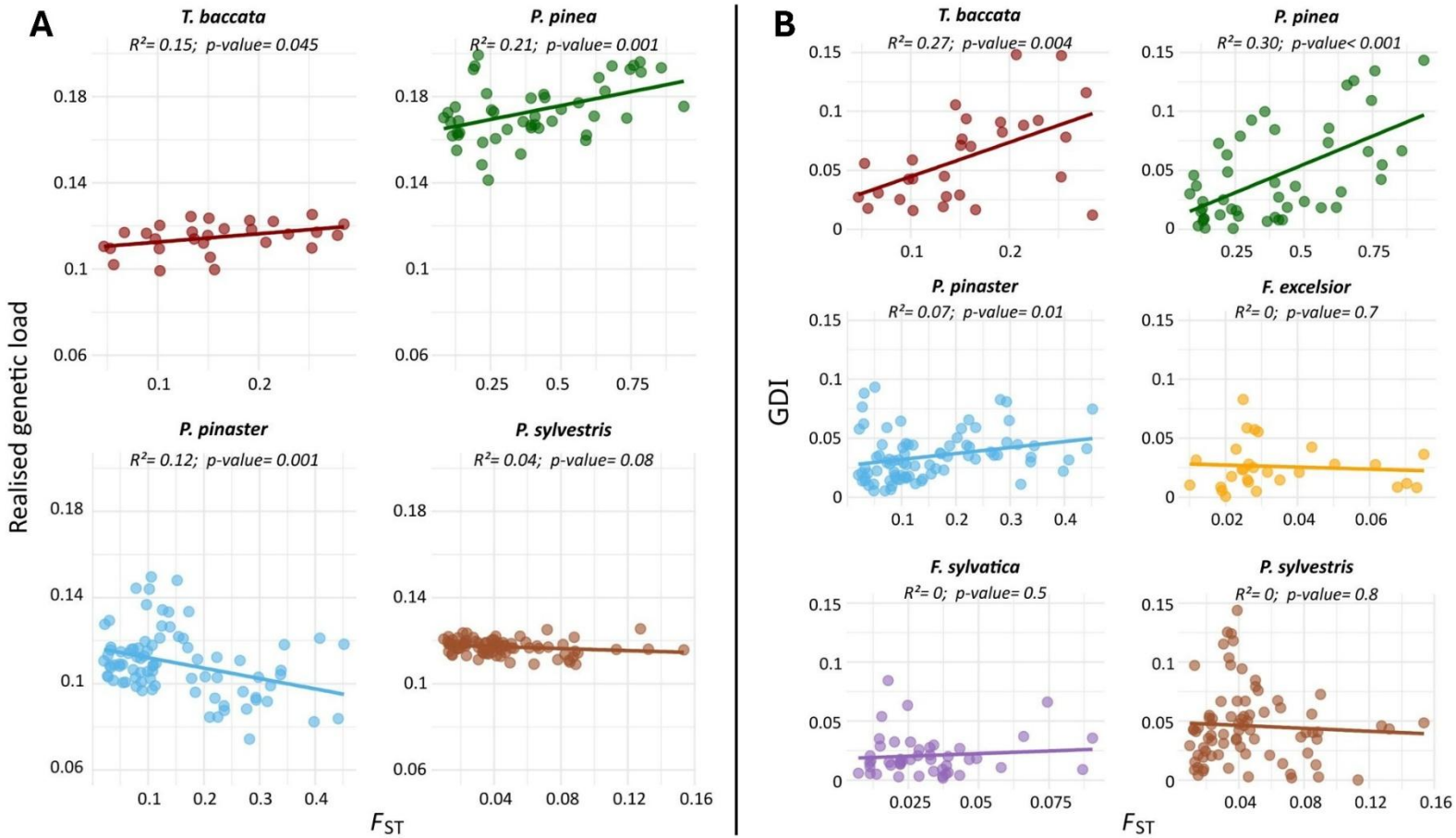

Figure 3. **Population-level genetic differentiation (F_{ST}) as a key factor explaining vulnerability to climate change.** Linear relationships between (**A**) realised genetic load (only conifers) or (**B**) GDI, and population-level F_{ST}, after excluding populations with atypically high F_{ST} values (see Methods and Fig. S5 for relationships including atypical populations). The coefficient of determination (R^2) and *F*-test *p*-values are shown for each model.

References

1. Brockerhoff, E. G. *et al.* Forest biodiversity, ecosystem functioning and the provision of ecosystem services. *Biodivers. Conserv.* **26**, 3005-3035 (2017).
2. Fréjaville, T., Vizcaíno-Palomar, N., Fady, B., Kremer, A. & Benito Garzón, M. Range margin populations show high climate adaptation lags in European trees. *Glob. Change Biol.* **26**, 484-495 (2020).
3. Petit-Cailleux, C. *et al.* Tree mortality risks under climate change in Europe: Assessment of silviculture practices and genetic conservation networks. *Front. Ecol. Evol.* **9**, 706414 (2021).
4. Martinez del Castillo, E. *et al.* Climate-change-driven growth decline of European beech forests. *Commun. Biol.* **5**, 163 (2022).
5. Forzieri, G. *et al.* Emergent vulnerability to climate-driven disturbances in European forests. *Nat. Commun.* **12**, 1081 (2021).
6. Taccoen, A., Piedallu, C., Seynave, I., Gégout-Petit, A. & Gégout, J.-C. Climate change-induced background tree mortality is exacerbated towards the warm limits of the species ranges. *Ann. For. Sci.* **79**, 23 (2022).
7. *Climate Change 2007: The Physical Science Basis*. (Cambridge university press, Cambridge, 2007).
8. Foden, W. B. *et al.* Climate change vulnerability assessment of species. *WIREs Clim. Change* **10**, e551 (2019).
9. Fitzpatrick, M. C. & Keller, S. R. Ecological genomics meets community-level modelling of biodiversity: Mapping the genomic landscape of current and future environmental adaptation. *Ecol. Lett.* **18**, 1-16 (2015).
10. Barratt, C. D. *et al.* Life on the edge: A new toolbox for population-level climate change vulnerability assessments. *Methods Ecol. Evol.* **15**, 2038-2058 (2024).
11. Lazic, D. *et al.* Genomic variation of European beech reveals signals of local adaptation despite high levels of phenotypic plasticity. *Nat. Commun.* **15**, 8553 (2024).

12. Ørsted, M., Hoffmann, A. A., Sverrisdóttir, E., Nielsen, K. L. & Kristensen, T. N. Genomic variation predicts adaptive evolutionary responses better than population bottleneck history. *PLoS Genet.* **15**, e1008205 (2019).
13. Leimu, R. & Fischer, M. A meta-analysis of local adaptation in plants. *PLoS ONE* **3**, e4010 (2008).
14. Marcora, P. I. *et al.* Are populations of *Polylepis australis* locally adapted along their elevation gradient? *Neotrop. Biodivers.* **7**, 246-256 (2021).
15. Browne, L., Wright, J. W., Fitz-Gibbon, S., Gugger, P. F. & Sork, V. L. Adaptational lag to temperature in valley oak (*Quercus lobata*) can be mitigated by genome-informed assisted gene flow. *Proc. Nat. Acad. Sci. USA* **116**, 25179-25185 (2019).
16. De Kort, H. *et al.* Pre-adaptation to climate change through topography-driven phenotypic plasticity. *J. Ecol.* **108**, 1465-1474 (2020).
17. Francisco, T. *et al.* Genomic signatures of climate-driven (mal)adaptation in an iconic conifer, the english yew (*Taxus baccata* L.). *Evol. Appl.* **18**, e70160 (2025).
18. Kardos, M., Taylor, H. R., Ellegren, H., Luikart, G. & Allendorf, F. W. Genomics advances the study of inbreeding depression in the wild. *Evol. Appl.* **9**, 1205-1218 (2016).
19. Pyhäjärvi, T., Kujala, S. T. & Savolainen, O. 275 years of forestry meets genomics in *Pinus sylvestris*. *Evol. Appl.* **13**, 11-30 (2020).
20. Cheptou, P.-O. The evolutionary ecology of inbreeding depression in wild plant populations and its impact on plant mating systems. *Front Plant Sci.* **15**, 1359037 (2024).
21. Lande, R., Schemske, D. W. & Schultz, S. T. High inbreeding depression, selective interference among loci, and the threshold selfing rate for purging recessive lethal mutations. *Evolution* **48**, 965-978 (1994).
22. Williams, C. G. & Savolainen, O. Inbreeding depression in conifers: Implications for breeding strategy. *For. Sci.* **42**, 102-117 (1996).
23. Olson-Manning, C. F., Wagner, M. R. & Mitchell-Olds, T. Adaptive evolution: Evaluating empirical support for theoretical predictions. *Nat. Rev. Genet.* **13**, 867-877 (2012).

24. Peischl, S., Dupanloup, I., Kirkpatrick, M. & Excoffier, L. On the accumulation of deleterious mutations during range expansions. *Mol. Ecol.* **22**, 5972-5982 (2013).

25. Peischl, S. & Excoffier, L. Expansion load: Recessive mutations and the role of standing genetic variation. *Mol. Ecol.* **24**, 2084-2094 (2015).

26. Ellegren, H. & Galtier, N. Determinants of genetic diversity. *Nat. Rev. Genet.* **17**, 422-433 (2016).

27. González-Martínez, S. C., Ridout, K. & Pannell, J. R. Range expansion compromises adaptive evolution in an outcrossing plant. *Curr. Biol.* **27**, 2544-2551.e4 (2017).

28. Hewitt, G. The genetic legacy of the Quaternary ice ages. *Nature* **405**, 907-913 (2000).

29. Star, B. & Spencer, H. G. Effects of genetic drift and gene flow on the selective maintenance of genetic variation. *Genetics* **194**, 235-244 (2013).

30. Milesi, P. *et al.* Resilience of genetic diversity in forest trees over the Quaternary. *Nat. Commun.* **15**, 8538 (2024).

31. Atkins, K. E. & Travis, J. M. J. Local adaptation and the evolution of species' ranges under climate change. *J. of Theor. Biol.* **266**, 449-457 (2010).

32. Kremer, A. *et al.* Long-distance gene flow and adaptation of forest trees to rapid climate change. *Ecol. Lett.* **15**, 378-392 (2012).

33. Tigano, A. & Friesen, V. L. Genomics of local adaptation with gene flow. *Mol. Ecol.* **25**, 2144-2164 (2016).

34. Bataillon, T. & Kirkpatrick, M. Inbreeding depression due to mildly deleterious mutations in finite populations: Size does matter. *Genet. Res.* **75**, 75-81 (2000).

35. Glémin, S. How are deleterious mutations purged? Drift versus nonrandom mating. *Evolution* **57**, 2678-2687 (2003).

36. Rogers, R. L. & Slatkin, M. Excess of genomic defects in a woolly mammoth on Wrangel island. *PLoS Genet.* **13**, e1006601 (2017).

37. Grossen, C., Guillaume, F., Keller, L. F. & Croll, D. Purging of highly deleterious mutations through severe bottlenecks in Alpine ibex. *Nat. Commun.* **11**, 1001 (2020).

38. Hasselgren, M. *et al.* Genomic and fitness consequences of inbreeding in an endangered carnivore. *Mol. Ecol.* **30**, 2790-2799 (2021).

39. Theraroz, A. *et al.* The genetic consequences of population marginality: A case study in maritime pine. *Divers. Distrib.* **30**, e13910 (2024).

40. Dubreuil, M. *et al.* Genetic effects of chronic habitat fragmentation revisited: Strong genetic structure in a temperate tree, *Taxus baccata* (Taxaceae), with great dispersal capability. *Am. J. Bot.* **97**, 303-310 (2010).

41. Burgarella, C. *et al.* Recent population decline and selection shape diversity of taxol-related genes. *Mol. Ecol.* **21**, 3006-3021 (2012).

42. Jaramillo-Correa, J. P. *et al.* Evolutionary rate and genetic load in an emblematic Mediterranean tree following an ancient and prolonged population collapse. *Mol. Ecol.* **29**, 4797-4811 (2020).

43. Alberto, F. J. *et al.* Potential for evolutionary responses to climate change - evidence from tree populations. *Glob. Change Biol.* **19**, 1645-1661 (2013).

44. Magri, D. Patterns of post-glacial spread and the extent of glacial refugia of European beech (*Fagus sylvatica*). *J. Biogeogr.* **35**, 450-463 (2008).

45. Magri, D. *et al.* A new scenario for the Quaternary history of European beech populations: Palaeobotanical evidence and genetic consequences. *New Phytol.* **171**, 199-221 (2006).

46. Heuertz, M. *et al.* Nuclear microsatellites reveal contrasting patterns of genetic structure between western and southeastern European populations of the common ash (*Fraxinus excelsior* L.). *Evolution* **58**, 976-988 (2004).

47. Heuertz, M. *et al.* Chloroplast DNA variation and postglacial recolonization of common ash (*Fraxinus excelsior* L.) in Europe. *Mol. Ecol.* **13**, 3437-3452 (2004).

48. Tollefsrud, M. M. *et al.* Genetic structure in the northern range margins of common ash, *Fraxinus excelsior* L. *PLoS ONE* **11**, e0167104 (2016).

49. Postolache, D. *et al.* Genetic signatures of divergent selection in European beech (*Fagus sylvatica* L.) are associated with the variation in temperature and precipitation across its distribution range. *Mol. Ecol.* **30**, 5029-5047 (2021).

50. Tyrmi, J. S. *et al.* Genomics of clinal local adaptation in *Pinus sylvestris* under continuous environmental and spatial genetic setting. *G3 (Bethesda)* **10**, 2683-2696 (2020).

51. Hurme, P., Repo, T., Savolainen, O. & Pääkkönen, T. Climatic adaptation of bud set and frost hardiness in Scots pine (*Pinus sylvestris*). *Can. J. For. Res.* **27**, 716-723 (1997).

52. Sánchez de Dios, R. *et al. Fagus sylvatica* L. Peripheral populations in the Mediterranean Iberian Peninsula: Climatic or anthropic relicts? *Ecosystems* **24**, 211-226 (2021).

53. Guadaño-Peyrot, C. *et al.* Genetic signatures of population marginality in four European conifers. In preparation.

54. Gómez, A., Vendramin, G. G., González-Martínez, S. C. & Alía, R. Genetic diversity and differentiation of two Mediterranean pines (*Pinus halepensis* Mill. and *Pinus pinaster* Ait.) along a latitudinal cline using chloroplast microsatellite markers. *Divers. Distrib.* **11**, 257-263 (2005).

55. Cheddadi, R. *et al.* Imprints of glacial refugia in the modern genetic diversity of *Pinus sylvestris*. *Glob. Ecol. Biogeogr.* **15**, 271-282 (2006).

56. Naydenov, K., Senneville, S., Beaulieu, J., Tremblay, F. & Bousquet, J. Glacial vicariance in Eurasia: Mitochondrial DNA evidence from Scots pine for a complex heritage involving genetically distinct refugia at mid-northern latitudes and in Asia Minor. *BMC Evol. Biol.* **7**, 233 (2007).

57. Mayol, M. *et al.* Adapting through glacial cycles: Insights from a long-lived tree (*Taxus baccata*). *New Phytol.* **208**, 973-986 (2015).

58. Wachowiak, W., Perry, A., Zaborowska, J., González-Martínez, S. C. & Cavers, S. Admixture and selection patterns across the European distribution of Scots pine, *Pinus sylvestris* (Pinaceae). *Bot. J. Linn. Soc.* **200**, 416-432 (2022).

59. Petit, R. J. *et al.* Glacial refugia: Hotspots but not melting pots of genetic diversity. *Science* **300**, 1563-1565 (2003).

60. Temunović, M. *et al.* Environmental heterogeneity explains the genetic structure of continental and mediterranean populations of *Fraxinus angustifolia* Vahl. *PLoS ONE* **7**, e42764 (2012).

61. Potter, K. M., Campbell, A. R., Josserand, S. A., Nelson, C. D. & Jetton, R. M. Population isolation results in unexpectedly high differentiation in Carolina hemlock (*Tsuga caroliniana*), an imperiled southern Appalachian endemic conifer. *Tree Genet. Genomes* **13**, 105 (2017).

62. Barrett, R. D. H. & Schluter, D. Adaptation from standing genetic variation. *Trends Ecol. Evol.* **23**, 38-44 (2008).

63. Eyre-Walker, A. & Keightley, P. D. The distribution of fitness effects of new mutations. *Nat. Rev. Genet.* **8**, 610-618 (2007).

64. Chen, J., Glémin, S. & Lascoux, M. Genetic diversity and the efficacy of purifying selection across plant and animal species. *Mol. Biol. Evol.* **34**, 1417-1428 (2017).

65. Dussex, N., Morales, H. E., Grossen, C., Dalén, L. & Oosterhout, C. van. Purging and accumulation of genetic load in conservation. *Trends Ecol. Evol.* **38**, 961-969 (2023).

66. Xue, Y. *et al.* Mountain gorilla genomes reveal the impact of long-term population decline and inbreeding. *Science* **348**, 242-245 (2015).

67. Feng, Y. *et al.* Genome sequences and population genomics provide insights into the demographic history, inbreeding, and mutation load of two 'living fossil' tree species of Dipteronia. *Plant J.* **117**, 177-192 (2024).

68. Bruxaux, J. *et al.* Scots pine - panmixia and the elusive signal of genetic adaptation. *New Phytol.* **243**, 1231-1246 (2024).

69. Slotte, T., Foxe, J. P., Hazzouri, K. M. & Wright, S. I. Genome-wide evidence for efficient positive and purifying selection in *Capsella grandiflora*, a plant species with a large effective population size. *Mol. Biol. Evol.* **27**, 1813-1821 (2010).

70. García-Dorado, A. Understanding and predicting the fitness decline of shrunk populations: Inbreeding, purging, mutation, and standard selection. *Genetics* **190**, 1461-1476 (2012).

71. Hedrick, P. W. & Garcia-Dorado, A. Understanding inbreeding depression, purging, and genetic rescue. *Trends Ecol. Evol.* **31**, 940-952 (2016).

72. Sexton, J. P., Strauss, S. Y. & Rice, K. J. Gene flow increases fitness at the warm edge of a species' range. *Proc. Nat. Acad. Sci. USA* **108**, 11704-11709 (2011).

73. Bontrager, M. & Angert, A. L. Gene flow improves fitness at a range edge under climate change. *Evol. Lett.* **3**, 55-68 (2019).

74. Frankham, R. Genetic rescue of small inbred populations: Meta-analysis reveals large and consistent benefits of gene flow. *Mol. Ecol.* **24**, 2610-2618 (2015).

75. Rellstab, C., Dauphin, B. & Exposito-Alonso, M. Prospects and limitations of genomic offset in conservation management. *Evol. Appl.* **14**, 1202-1212 (2021).

76. Aitken, S. N. & Bemmels, J. B. Time to get moving: Assisted gene flow of forest trees. *Evol. Appl.* **9**, 271-290 (2016).

77. Pinosio, S. *et al.* The FORGENIUS Genomic Resources: New Genotyping Tools and Genomic Data for 23 Forest Tree Species and Their Genetic Conservation Units. *Mol. Ecol. Resour.* **26**, e70115 (2026).

78. Budde, K. B., Doonan, J.M., Hanika, T., Verbylaite, R., Ulaszewski, B. , Kjær E.D., Heuertz, M., Nielsen, L.R. Evolutionary consequences of ash dieback in natural common ash populations in Europe. In preparation.

79. Doonan, J. M. *et al.* Multiple, single trait GWAS and supervised machine learning reveal the genetic architecture of *Fraxinus excelsior* tolerance to ash dieback in Europe. *Plant Cell Environ.* **48**, 3793-3809 (2025).

80. Meger, J., Ulaszewski, B., Pałucka, M., Kozioł, C. & Burczyk, J. Genomic prediction of resistance to Hymenoscyphus fraxineus in common ash (*Fraxinus excelsior* L.) populations. *Evol. Appl.* **17**, e13694 (2024).

81. Bajc, M. *et al. Fagus sylvatica* BU2012: A genetic dataset for trial trees from the international beech provenance trial 'Kamenski hrib/Straža (SI) 1996/1998'.

https://dirros.openscience.si/IzpisGradiva.php?id=27722&lang=eng (2026) doi:10.20315/Data.0014.

82. Olsson, S. *et al.* Genetic assignment at different geographical levels: A case study in a forest tree species (*Pinus pinaster* Ait.) using SNP markers. *Evol. Appl.* **18**, e70145 (2025).
83. Olsson, S. *et al.* Range-wide SNP reference data and filtering effects in three major European pines. In preparation.
84. Linck, E. & Battey, C. J. Minor allele frequency thresholds strongly affect population structure inference with genomic data sets. *Mol. Ecol. Resour.* **19**, 639-647 (2019).
85. Niu, S. *et al.* The Chinese pine genome and methylome unveil key features of conifer evolution. *Cell* **185**, 204-217.e14 (2022).
86. Xiong, X. *et al.* The *Taxus* genome provides insights into paclitaxel biosynthesis. *Nat. Plants* **7**, 1026-1036 (2021).
87. Marchi, M., Bucci, G., Iovieno, P. & Ray, D. ClimateDT: A global scale-free dynamic downscaling portal for historic and future climate data. *Environments* **11**, 82 (2024).
88. Metheringham, C. L. *et al.* Rapid polygenic adaptation in a wild population of ash trees under a novel fungal epidemic. *Science* **388**, 1422-1425 (2025).
89. Oksanen, J. *et al.* vegan: Community Ecology Package. 2.6-8 https://doi.org/10.32614/CRAN.package.vegan (2025).
90. Olsson, S., Jaramillo-Correa, J. P., Vajana, E., Pinosio, S., Macaya-Sanz, D., Bagnoli, F., Avanzi, C., Piotti, A., Alía, R., Mutke, S., Vendramin, G. G., Grivet, D., González-Martínez, S. C. Thriving with low diversity: demographic history and evolutionary dynamics of stone pine (*P. pinea* L). In preparation.
91. Pritchard, J. K., Stephens, M. & Donnelly, P. Inference of population structure using multilocus genotype data. *Genetics* **155**, 945-959 (2000).
92. Evanno, G., Regnaut, S. & Goudet, J. Detecting the number of clusters of individuals using the software STRUCTURE: A simulation study. *Mol. Ecol.* **14**, 2611-2620 (2005).

93. Savolainen, O., Pyhäjärvi, T. & Knürr, T. Gene flow and local adaptation in trees. *Annu. Rev. Ecol., Evol. Syst.* **38**, 595-619 (2007).

94. Kitada, S., Nakamichi, R. & Kishino, H. Understanding population structure in an evolutionary context: Population-specific FST and pairwise FST. *G3: Genes Genomes Genet.* **11**, jkab316 (2021).

95. Foll, M. & Gaggiotti, O. A genome-scan method to identify selected loci appropriate for both dominant and codominant markers: A bayesian perspective. *Genetics* **180**, 977-993 (2008).

96. Nei, M. *Molecular Evolutionary Genetics*. (Columbia University Press, 1987). doi:10.7312/nei-92038.

97. Piñeiro, R. *et al.* A higher load of deleterious mutations has a detrimental effect on tree growth in maritime pine. 2025.11.09.687477 Preprint at https://doi.org/10.1101/2025.11.09.687477 (2025).

98. Cingolani, P. *et al.* A program for annotating and predicting the effects of single nucleotide polymorphisms, SnpEff. *Fly* **6**, 80-92 (2012).

99. Choi, Y. & Chan, A. P. PROVEAN web server: A tool to predict the functional effect of amino acid substitutions and indels. *Bioinformatics* **31**, 2745-2747 (2015).

100. Archambeau, J. *et al.* Evaluating genomic offset predictions in a forest tree with high population genetic structure. *Am. Nat.* 000-000 (2025).

101. Warnes, G. genetics: Population Genetics. 1.3.8.1.3 https://doi.org/10.32614/CRAN.package.genetics (2012).

102. R Core Team. R: A language and environment for statistical computing. *R Foundation for Statistical Computing, Vienna, Austria* (2023).

103. Caudullo, G., Welk, E. & San-Miguel-Ayanz, J. Chorological maps for the main European woody species. *Data Br.* **12**, 662-666 (2017).